Coupling of Surface-Plasmon Polariton in nano-arrays of particles

P. Segovia[1] , *R. Cortes*[2], *C. Garcia*[1], *N. Elizondo*[1] and *V.Coello*[2]

[1]Unidad Monterrey CICESE, Alianza Sur 203, Autopista al Aeropuerto Km 10, PIIT CP 66600 Apodaca, NL Mexico.

[2]Doctorado en Ingeniería Física Industrial, FCFM UANL. Pedro de Alba S/N Ciudad Universitaria, S.N. de Los G. NL, Mexico.

Keywords: Surface plasmons polaritons, Plasmonics, Nanoparticles, Green´s function method

Abstract

We investigate numerically the possibility of simultaneous surface plasmon-polariton (SPP) excitation and in-plane manipulation by using arrays of nanoparticles. The SPP excitation followed by refraction, focusing and waveguiding of SPP waves is simulated with nanoparticle arrays of different shapes, demonstrating the feasibility of the suggested approach. The calculations are based in a relative simple vectorial dipolar model for multiple SPP scattering [T. Søndergaard and S.I. Bozhevolnyi, "Vectorial model for multiple scattering by surface nanoparticles via surface polariton-to-polariton interactions", Phys. Rev. B Vol. 67, No 16, 165405-165412, 2003].

1. Introduction

Surface Plasmon Polaritons (SPPs) are collective electron oscillations localized at the surface of metal-dielectric structures. The unique optical properties of SPPs [1] open promising technological perspectives within nano-optics, e.g., for miniaturization of photonics circuits with length scales much smaller than currently achievable, inter-chip and intra-chip applications in computer systems, and bio/sensor-systems [2-4]. In particular, metallic nanoparticle arrays played an important role for the development of novel plasmonic structures [5]. In this context, extensive theoretical studies have been conducted. The theoretical framework, however, is not trivial, since even the SPP scattering due to a single circular nano-particle requires elaborated numerical simulations [6]. A relative simple dipole scattering approach for light scattering from a random array of nanoparticles

was developed [7]. There, the authors deal with the randomness in particle positions by convolving the single-particle Green´s dyadic with a correlation function that describes the average properties of the particle distribution. Furthermore, a similar numerical approach has been used to calculate SPP scattering produced by band-gap structures [8] and model the operation of a plasmonic interferometer [9]. Recently, this model was further developed [10] and applied to the problem of SPP guiding by chains of strongly interacting nanoparticles [11]. Here, one should bear in mind that, for any plasmonic devices, the issue of SPP excitation with free-propagating optical radiation has to be considered. Conventionally, most of SPP excitations methods are based on the use of glass prisms as couplers [1]. This approach has some drawbacks such as the separation of the source and plasmonic devices on different chips, and the large size of the prism couplers that make them not suitable for photonic integrated circuits. An alternative is the use of a normal incident light to excite the SPPs through a ridge [12] or subwavelength- hole arrays [13] located at the top of an air/metal interface. Such SPP launching mechanism has been used for quantitative experimental analysis of a SPP interferometer [14], nano-parabolic chains [15], and testing of refractive plasmonic structures [16]. Here, using a vectorial dipolar model for multiple SPP scattering [7, 8], we investigate the feasibility of exciting and manipulating SPPs without using external excitation elements. The possibility of a simultaneous process of SPP excitation and propagation control is elucidated by using periodic square arrays of nanoparticle illuminated by a normally incident Gaussian beam. The system is expected to work as, both, the launching mechanism and the plasmonic element itself. Direct SPP excitation on plasmonic elements may open opportunities for realizing photonic circuits or components with high compactness. SPP refraction, focusing and waveguiding are demonstrated with different (in shape) nano-arrays, exhibiting features that closely resembled some experimental results for SPP scattering on nanostructures [16, 17]. It should be noted that the light-SPP coupling efficiency in this configuration is expected to be similar to that of a rectangular ridge, since an array of nano-particles in the limit of vanishingly small inter-particle distances should exhibit the scattering properties that are similar to those of a continuous rectangular ridge. Experimental and theoretical investigations of SPP excitation with individual ridges indicated that the overall excitation efficiency for 350-nm-wide and 130-nm-high gold

ridges can reach 7% at the free-space wavelength of 800 nm [18]. For our configuration, the direct evaluation of the optimum SPP coupling efficiency using the vectorial dipolar model is cumbersome and typically omitted [19], since it should involve, among other things, a careful analysis of strong particle-surface interactions whose accurate description might require to go beyond the framework of dipole scattering approach [8]. We would like to emphasize that the main idea of the proposed approach is in avoiding the usage (in plasmonic circuits utilizing control of SPP propagation by surface nanostructures) of additional interfacing elements such as, for example, in-coupling ridges and focusing elements.

2. The model

The numerical model is based on the following. When light is incident on a metal/dielectric interface with scattering objects, the objects can be modelled as point-like dipoles. This assumption leads to the construction of an approximate Green´s tensor describing the SPP scattering by such dipoles. The validity of the model is established for relatively large inter-particle distances ($>\lambda_0/2$) whereas for smaller distances one has to include multipolar contributions in the scattered field [8]. Thus, the polarization of the i'th scaterer takes the form:

$$P_i = \alpha \cdot E_0(r_i) + \frac{k_0^2}{\varepsilon_0} \sum \alpha \cdot G(r_i, r_n) \cdot P_n \quad , \qquad (1)$$

where α is the polarizability of the scatterers, $E_0(r_i)$ is the incident field at the site of scatterer i, k_0 is the wave vector of the incoming field in the space, $G(r_i, r_n)$ the Green tensor for SPP to SPP scattering (total field propagator) [8]. The Green tensor is the sum of a direct contribution, $\boldsymbol{G^d}$, in this case the free space Green´s tensor, and an indirect contribution, $\boldsymbol{G^S}$, that describes both reflection from the metal/dielectric interface and excitation of SPPs. Here the polarizability α has the surface dressing included *i.e.* the coupling of the dipole to itself through reflection in the surface. Futhermore, the polarizability, α, is a tensor, describing the polarizability effect in each direction [8]:

$$\alpha = \left(I - k_0^2 \frac{\alpha_0}{\varepsilon_0} \cdot G^S(r,r') \right)^{-1} \cdot \alpha^0 \quad . \tag{2}$$

Where α_0 is the free space polarizability tensor given as

$$\alpha^0 = \varepsilon_0 I 4\pi a^3 \frac{\varepsilon_2 - 1}{\varepsilon_2 + 2}, \tag{3}$$

with I being the unit dyadic tensor. Equation (2) is valid when the long-wavelength electrostastic approximation has been used. Such approximation assumes that the field is constant within the considered range, which corresponds to the size of the scatterer. For the approximation to be valid, the wavelength must be much bigger than the size of the scatterer. If the image dipole approximation is used on $G^S(r,r')$ in Eq. (2) the following result is obtained for the polarizability tensor of Eq. (1).

$$\alpha \approx \left[\frac{\varepsilon_2 - 1}{\varepsilon_2 + 1} \cdot \frac{\varepsilon_2 - 1}{\varepsilon_2 + 2} \left(\frac{1}{8} \hat{x}\hat{x} + \frac{1}{8} \hat{y}\hat{y} + \frac{1}{4} \hat{z}\hat{z} \right) \right]^{-1} \cdot \alpha^0 \quad . \tag{4}$$

It should be mentioned that the dipole approximation assumes that the phase delay of the field, when it moves over the scatterer, is negligible. Mathematically this means $e^{k \cdot r} \cong 1$ for a given field. This means again that the size of the scatterer should be smaller than the wavelength, which is the main assumption in the model. When Eq. (4) has been used in Eq. (1) to determine the polarization, the final step is to calculate the field outside the scatterer as a selfconsistent field:

$$E(r) = E^0(r) + \frac{k_0^2}{\varepsilon_0} \sum_n G(r,r') \cdot P_n \quad . \tag{5}$$

The complete analysis and validity of the model is beyond the scope of this report and can be found elsewhere [8].

3. Numerical results

Following a step-by-step process, first we calculate the in-plane scattered field created by a normally incident Gaussian beam (λ_0=750 nm, FWHM=5μm, *x*-pol) of unit amplitude impinging on a 150-nm-period square lattice (width $w \approx 1.05$ μm, length $L \approx 15$μm) of nanoparticles with radius, *r*, of 20 nm (Fig. 1(a,b)). The entire system is simulated on a gold surface with dielectric constant ε=-23.11+1.4i. Fig. 1(b) shows numerical simulations of a direct SPP excitation taking place at the left (along *x*-axis) nanoarray edge. Hereafter, for all images, the total field is calculated 80 nm above the air-gold interface, and the incident beam has been removed; *i.e*; only scattered SPP appear in the pictures. Fig. 1(c) shows the power of the SPP beam propagating in the positive direction of *x*-axis calculated as a function of the incident beam position (along the *x*-axis). One can notice that once the incident beam is not in contact with the nanoarray, the optical power is weak (Fig. 1(c)); this is expected, considering that no SPP can be launched without interacting with the nanoarray. Once the launching of SPP is achieved, in this way, from an application point of view, one can exploit the nanoarrays in order to manipulate the SPP propagation. A nanodevice, realizable by a certain array structure, is a nano-prism. The concept is to place a 150-nm-period triangular array of gold nanoparticles on top of a flat gold surface in order to simulate a bidimensional right-prism (Fig. 2(a)). Direct SPP excitation is achieved at the first prism structural edge (Fig. 2(b)) where no refraction is expected to occur. The second prism edge is hit at oblique incidence and, there, the SPP propagation direction is changed due to refraction effects as it happens with a light beam passing through a glass prism (Fig. 2(b)). SPP mode propagating inside the nano-prism experiences an increase in the effective refractive index (ERI) with respect to that of a flat surface. By measuring the deflection of the transmitted beam (≈3 degrees) and by applying Snell´s law, the ERI refractive index could be determined to be neff ≈ 1.05, which is in good agreement with the experimental value of [16]. A set of prisms with their angles, particularly near the edges, being larger than 45 degrees can be seen as a circular-shaped periodic array. Figure 3 (a-c) illustrates the

focusing of plasmons by a semi-spherical lens of 7.5 μm diameter at different free-space wavelenghts. One can also notice that neither of the figures shows a SPP focusing to a spot. This has two reasons: (i) the incident SPP beam is not plane, but more a divergent Gaussian beam, and (ii) there is a sufficient spherical aberration due to the nonparaxial rays participating in the image formation. Scattering of the plasmons at nanoparticle arrays also enables guiding of the SPPs. A particularly simple geometry of a plasmonic waveguide is presented in Fig. 4(a,b). The waveguide consists of a periodic square-shaped nanoarray of $w \approx 2$ μm and $L \approx 12$μm. We launched plasmons by illuminating, with a normally incident Gaussian beam (λ_0 = 750 nm, FWHM = 2 μm, *x*-pol), the low corner of the left-end of the nanoarray (Fig. 4(a)). The SPP waveguiding capability is evidenced by the SPP beam coming out of the waveguide (Fig. 4(a)). Note that, in Fig 4(a), one can observe how the SPP is confined in the waveguide by multiple total internal reflections. By doing so, the SPP mode can be transported from one waveguide end to another one. In contrast, SPP waveguiding is almost not observed when the incident beam is placed on the midsection of the nanoarray (Fig. 4(b)). At the midsection, the nanoarray is almost symmetric over the extent of the incident beam and therefore cannot scatter efficiently in the axial direction since the incoming propagating vector and the propagating SPP vector are hardly matched. However, this symmetry is broken at the nanoarrays ends where light is scattered into propagating SPP modes. Likewise, propagating SPP modes are excited in thin-film surface utilizing gratings or dots.

4. Conclusion

Using nano-particles arrays, the feasibility of simultaneous excitation, propagation and manipulation of SPP fields was corroborated. The numerical calculations were carried out by using a relatively simple vectorial dipolar model for multiple SPP scattering [8] that allows one to explicitly formulate the set of linear equations for the self-consistent field, facilitating greatly computer aided design considerations. Plasmonic prisms, lens and waveguides were studied by using several system parameters as different free wavelengths and incident beam positions. The results show the feasibility to manipulate SPPs without using external excitation elements as for example an in-coupling ridge. In order to explore more this possibility further theoretical and experimental works are needed.

Acknowledgement

Two of us (R.C. and V.C.) acknowledge financial support from CONACyT Mexico, project No 123553.

References

[1]. (a) H. Raether, *Surface Plasmons*, Springer Tracts in Modern Physics, Springer, Berlin, 1988, vol. 111. (b) V.M. Agranovich, D.L. Mills (Eds.), *Surface Polaritons*, North-Holland, Amsterdam, 1982.

[2] Zia, R; Schuller, J.A; Brongersma, M.L. *Maters.Today*. 2006, Vol. 9, 20-27.

[3] Barnes, W.L; Dereux, A; Ebbesen, T.W. *Nature*, 2003, Vol. 424, 824-830.

[4] Ebbesen, T.W; Genet, C; Bozhevolnyi, S.I. *Phys. Today*. 2008, Vol. 61, 44–50.

.

[5] M L. Brongersma; P.G. Kik; (Eds.) *Surface Plasmon Nanophotonics*, 2007, Springer Berlin, Vol. 131.

[6] Shchegrov, A. V; Novikov, I. V; Maradudin, A. A; Phys. Rev. Lett. 1997. Vol. 78, 4269–4272.

[7] Soller, B. J; Hall, D. G. *J. Opt. Soc. Am. B*, 2002, Vol.19, 2437-2448.

[8] Søndergaard, T; Bozhevolnyi, S.I. *Phys. Rev. B*, 2003, Vol. 67, 165405-165412.

[9] Coello, V; Søndergaard, T; Bozhevolnyi, S.I. *Opt. Comm*, 2004, Vol. 240, 345-350.

[10] Evlyukhin, A.B; Bozhevolnyi, S.I. *Phys. Rev. B*, 2005.Vol. 71, 134304-134312.

[11] Evlyukhin, A.B; Bozhevolnyi, S.I. *Laser Phys. Lett*. 2006, Vol. 3, 396-400.

[12] Kim, D.S; Hohng, S.C; Malyarchuk, V; Yoon, Y.C; Ahn, Y.H; Yee, K.J; Park, J.W; Kim, J; Park, Q.H; Lienau, C; *Phys. Rev. Lett*. 2003, Vol. 91, 143901-143914.

[13] Devaux, E; Ebbesen, T.W; Weeber, J.-C; Dereux, A. *Appl. Phys. Lett*. 2003, Vol. 83, 4936-4938.

[14] Drezet, A; Hohenau, A; Stepanov, A.L; Ditlbacher, H; Steinberger, B; Aussenegg, F; Leitner, A; Krenn, J; *Plasmonics*, 2006, Vol. 1, 141-145.

[15]. I.P. Radko, S.I. Bozhevolnyi, A.B. Evlyukhin, A. Boltasseva, "Surface plasmon polariton beam focusing with parabolic nanoparticle chains", Opt. Exp. Vol. 15, No 11, 6576-6582, 2008.

[16] Radko, I.P; Evlyukhin, A.B; Boltasseva, A; Bozhevolnyi, S.I. *Opt. Exp*. 2008.Vol. 16, 3924-3930.

[17] Griesing, S; Englisch, A; Hartmann, U. *Journal of Physics: Conference Series*, 2007, Vol. 61, 364-368.

[18] Radko, I.P; Bozhevolnyi, S.I; Brucoli, G; Martín-Moreno, L; García-Vidal, F.J; Boltasseva, A. *Phys. Rev. B*, Vo. 78, 115115-,115121.

[19] Evlyukhin, A.B; Bozhevolnyi, S.I; Stepanov, A.L; Kiyan R; Reinhardt, C; Passinger, S; Chichkov B.N. *Opt. Exp*. 2007, Vol. 15, No 25, 16667-16680.

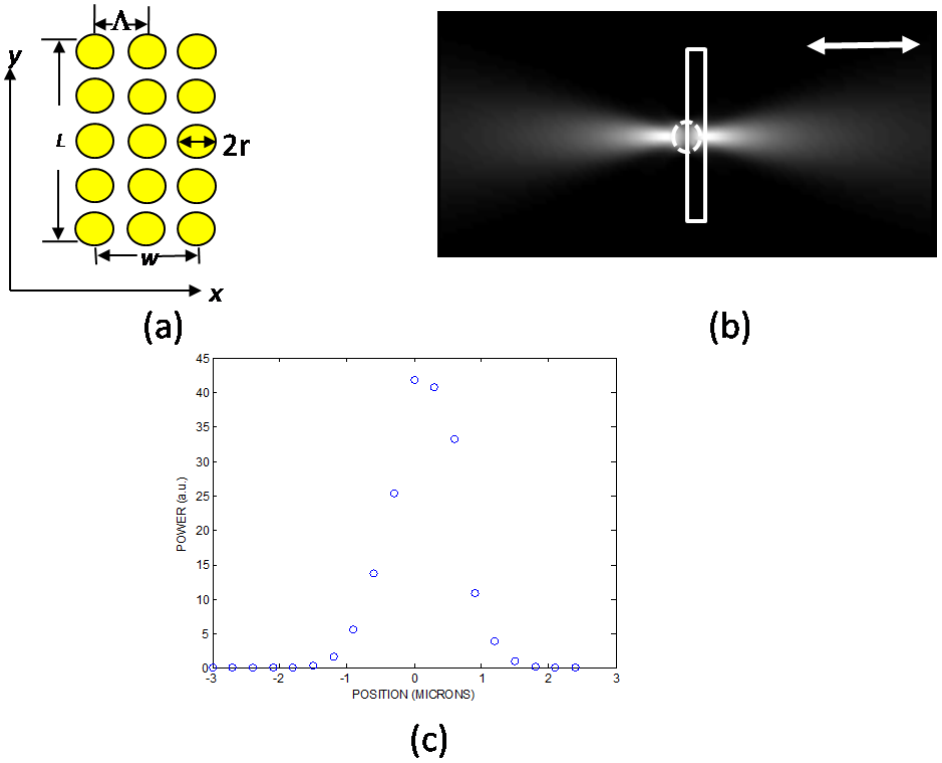

Fig. 1. (a) Schematic layout of a periodic square-lattice gold nanoparticle array, where r is the particle radius, *L*, *w*, and Λ are the array length, width, and period, respectively. (b) Electric field magnitude distribution (20 x 40 μm^2) calculated at the height of 80 nm above the air–gold interface for the incident (dotted circle) Gaussian light beam (wavelength, λ = 750 nm, FWHM = 5 μm, the polarization is along *x*-axis) being incident on the nanoarray (white rectangle). The lateral size of the nanoarray is 150 nm. (c) The power of the SPP beam propagating in the positive direction of *x*-axis calculated as a function of the incident beam position (along the *x*-axis). The white arrow in (b) indicates the incident light polarization.

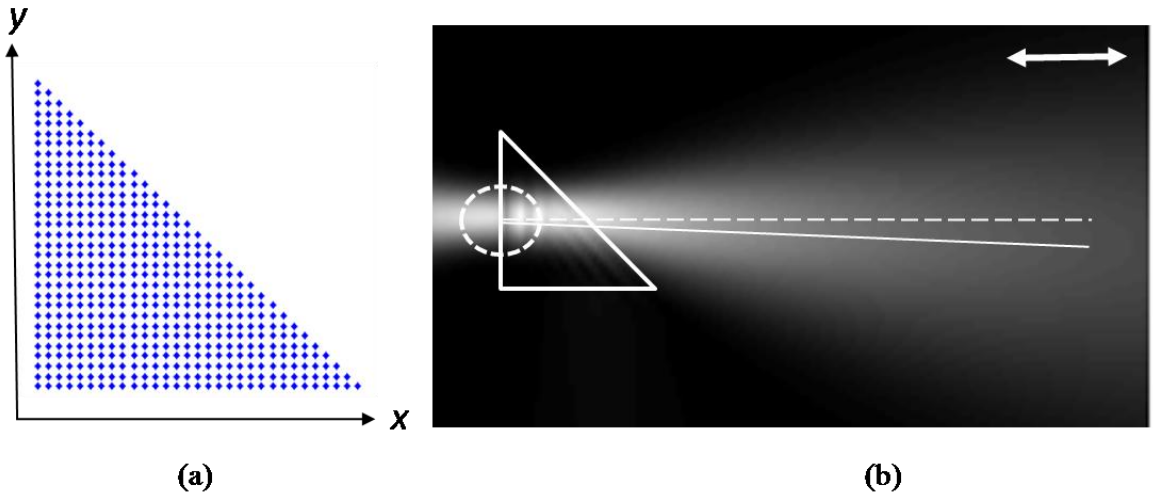

Fig 2. (a) Pictorial representation of the nanoprism (triangular nanoparticle array, r= 20 nm). (b) Electric field magnitude distribution (10 x 20 μm^2) calculated at the height of 80 nm above the air–gold interface for the incident (dotted circle) Gaussian light beam (wavelength, λ = 750 nm, FWHM = 3.5 μm, the polarization is along x-axis) being incident on the nanoarray (white triangle). SPP propagation direction is shown by a solid line. Dashed line shows the propagation direction of the SPP beam in a normal direction with respect to the first nanoprism edge. The white arrow in (b) indicates the incident light polarization.

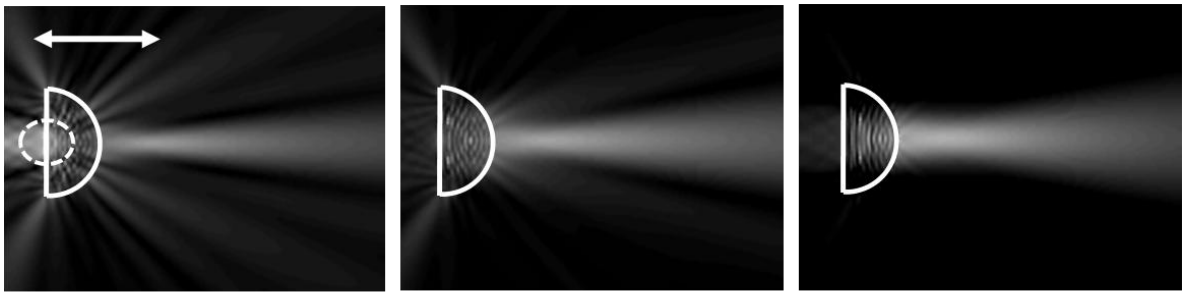

Fig 3. Electric field magnitude distribution (10 x 15 μm^2) calculated at the height of 80 nm above the air–gold interface for the incident (dotted circle) Gaussian light beam (FWHM = 2 μm) being incident on the semi-circular-shaped periodic structure of 7.5 μm-diameter (white semi-circle, r =20nm). The images were calculated at free-space wavelengths of (a) 730 nm, (b) 800 nm, and (c) 860 nm.

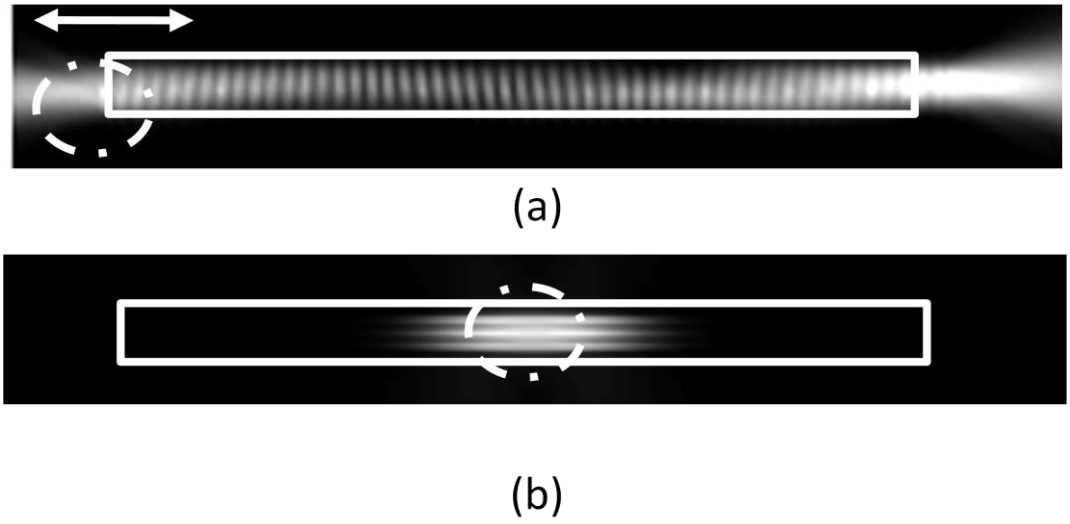

Fig. 4. Electric field magnitude distributions (2 x 30 μm^2) calculated for nanoarray waveguides with L = 12 μm, w = 2 μm, Λ= 200 nm, r=20nm, and for incident beam positions placed at (a) low corner of left entrance (b) midsection, The dotted circle represents the incident Gaussian beam (FWHM = 2 μm). The arrow indicates the incident light polarization in both cases.